



Nondestructive Evaluation of Iron-based Material by Using Magnetic Sensors

Koji Yamada¹⁾, Sinnichi Shoji¹⁾, Yoshiyuki Takeda¹⁾ and Yoshihiro Isobe²⁾

1) Graduated School of Saitama University, Japan

2) Nuclear Fuel Industries Ltd., Japan

ABSTRACT

Nondestructive evaluation of iron based material has been investigated by using a GaAs Hall element for magnetic leakage flux observation and by a pick-up coil for magnetic noise detection. We attained a high sensitivity down to 100 nT and a high spatial resolution as small as 200 μm , due to a short lift-off distance and a small sensor size of 120 μm . The residual stresses and the magnetic anisotropies in the Lüders band, were found broadly distributed at about 25-45 degrees against the direction of the applied stress. As a valid indicator of the material fatigue, average fields for discontinuous magnetizations were successfully derived by induced voltages in the pick-up coil as a function of sample positions and angles against the applied stress direction.

1. INTRODUCTON

Nowadays, the nondestructive evaluations (NDE) of structural material are of great importance for environmental problems of the society. It is especially important to inspect large scale structures e.g. tankers and nuclear power plants, far before the fatal errors. For these purposes, various methods of NDE have been investigated on iron- based material by observing ultrasonic propagation, X-ray diffraction, Vickers hardening etc. Recently, superconducting quantum interference device (SQUID) has been intensively investigated on the leakage flux or the spontaneous magnetization for nondestructive evaluation of material [1,2]. However SQUID is not appropriate for this purpose, due to the complex fabrication of the devices with cryogenic devices and careful treatments. In the present investigation, we developed diagnostic tools for the early warning system of the material degradation by using a conventional semiconductor Hall sensor, instead of SQUID, and a pick-up coil for magnetic noise detection. Material degradations or fatigues can be evaluated in connections with lattice imperfections in a microscopic term and/or residual stress in rather macroscopic term, for which magnetic properties are very sensitive. Therefore, we observed leakage flux distribution over a sample after a full polarization in a strong and uniform magnetic field, which enabled to detect the spatial inhomogeneity of the local degradation. We attained a high spatial resolution of degradation of about 200 μm with a small area Hall sensor. Further, magnetic noises (Barkhausen noise; BN) are also very sensitive to the lattice imperfection or directly affected by the pinning centers for magnetic domain shifts. BN's have been investigated on their spectra, intensities, or fractal dimensions as a function of the material degradations [3,4,5]. In this paper, a valid indicator of the residual stress or degradation at each position is derived by magnetic BN as a function of residual stresses observed by X-ray Diffractometer (XRD). We considered the validity of the indicator taking account of the nature of the induced voltages in the pick-up coil mounted at the sample surface. However, the indicator should have an insensitive property against the absolute BN amplitude in the pick coil mounted at some geometrically rough surfaces. For this postulation, we calculated

an expectation value of the average field for discontinuous magnetization by normalizing the voltages in the pick-up with total power of the voltages. The average field derived by this method is completely different from the former research work [3], where they directly obtained the absolute value of the mean square root of the induced voltages in a pick-up coil as a function of positions or of angles against the sample direction. The discussion on the average field was based on a model that the magnetic noises are generated by de-pining of the magnetic domain shift in a single grain and the pick-up coil can detect the flux change within a very small spatial distance for the separate each pulsed motions. Following this analysis, the relationship between the residual stress and the average field as a indicator at each position was numerically derived.

2. EXPERIMENTS

The low alloy steel of A533B ($Mn_{1.53}, Ni_{0.66}, C_{0.18}, Cu_{0.03}, Al, N, P, \dots$) were given by the Res. Inst. for Atomic Energy, Japan for Round Robin Tests composed of loading tests, TEM observations, Vickers tests, M-H curve, X-ray diffraction and the magnetic leakage observations at each loading condition. After annealing in at 600-650 C, the samples were applied stresses up to 640 MPa for the yield of 560 MPa of this material. The residual strains (ϵ) of No.1 and No.2 samples were 0.015 (540 MPa) and 0.14 (640MPa) for thickness deformations ($-\delta d/d$) of 0.08% and 0.17 %, respectively.

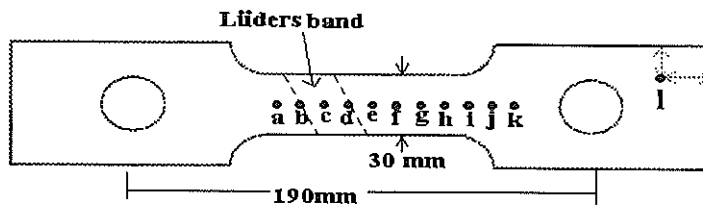


Fig.1 Typical shape of sample No.1 and 2 and the specific measuring points.

Fig. 1 shows the sample shape where measurement spots “a”-“l” are pointed for the various observations of leakage flux, residual strains by XRD and magnetic noises. The experiments of the leakage flux observations of these samples were performed by

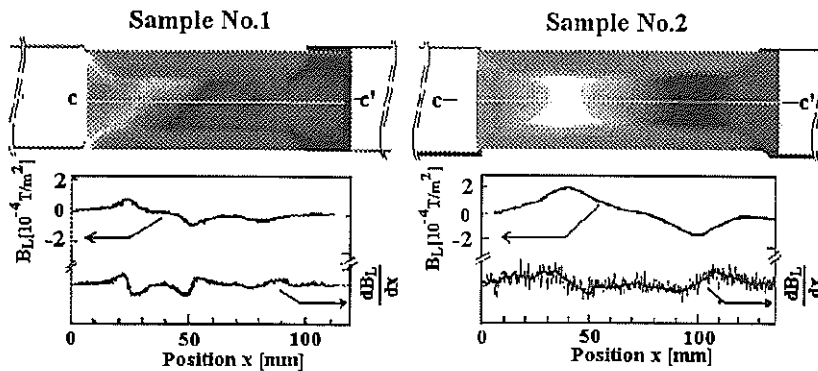


Fig. 2 The leakage flux distribution of the samples

Note: Leakage flux distribution is illustrated by B&W for incoming and out-going flux from surface.

using a GaAs Hall element of $120\ \mu\text{m} \times 120\ \mu\text{m}$ rectangular shape. The GaAs Hall element was operated in a frequency at 10 kHz for the lock-in operation to obtain a high signal to noise ratio. In this experiment, we attained a sensitivity down to 10^{-7} [T] in a term of 1 LSB (Least Significant Bit) for a 12 bit ADC. The signal voltages of leakage flux at each point were recorded up to 512×256 pixels over the sample area. The distributions of the leakage flux were observed after polarization in 1 kOe ($=80\text{kA/m}$), where the patterns of Lüders band appeared in the sample No.1 as shown by the zone in between the two broken lines in Fig. 1. Fig.2 shows the perpendicular component of leakage flux for sample No.1 and No.2, respectively. The upper pictures illustrate the leakage flux distribution in white and black colors where white color denotes the outwards leakage flux and black color for inwards flux. The lower figures illustrate the leakage flux intensity and their derivative with respect to the position x as a function of position x along the lines c - c' . The leakage flux intensity increased at the positions where residual stress begin increasing with position and vice versa.

Measurements of Barkhausen noises (BN) of the samples were observed by using a specially designed pick-up coil where a pick-up coil of 2mm located off-center between the two poles of the yoke, by which the output signals are always positive due to off-centers shown in Fig. 3. Externally applied fields were swept linearly with time elapse as $H(t) = ct$ ($c = 2.4 \times 10^4$ A/m·s) up to 1.6 kA/m as illustrated in the inset of Fig. 3. The electro-motive forces (emf) in the pick-up coil at a point R (e.g. "a"- "l") were recorded up to 16,000 points by an A/D converter (sampling rate of 1 μs /point, 1/4096 resolution). The signal profile is composed of sequential spikes of pulse duration of about 20 μs . Fig.4 and Fig.5 show the original traces of the emf ($V_D \sim dM/dH$) observed in different angles of the yoke against applied stress direction for the sample No.1 and those at different positions for the No.2, respectively.

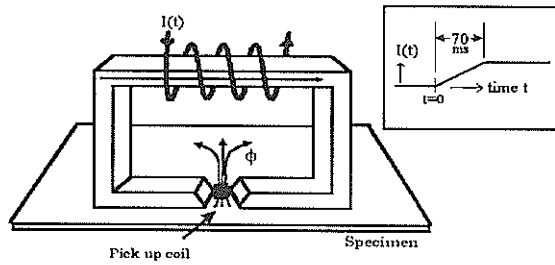


Fig.3 Experimental setup for the magnetic noise measurements

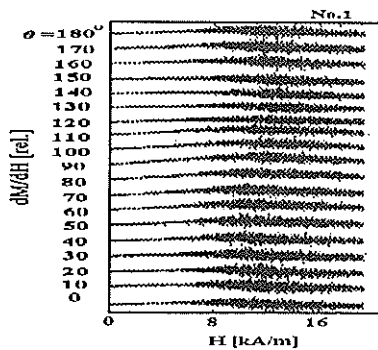


Fig.4 dM/dH vs. H for different angles for sample No.1 at a position "c" in Fig. 1

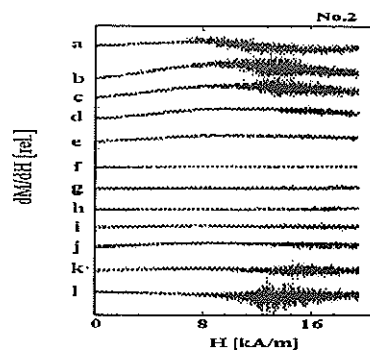


Fig. 5 dM/dH vs. H at different positions of "a"- "l" for No.2 sample.

The anisotropy at a position was obtained by tilting the yoke angles θ against the direction of the applied stress. We processed these signals $V_D(R, \theta, t)$ by a high pass filter with $t=1\text{ms}$, to eliminate the continuous signal caused by the continuous domain wall movements. After these processes, we derived an averaged magnetic field $\langle H_D(R, \theta, t) \rangle$ by using $V_D(R, \theta, t)$ defined as follows.

$$\begin{aligned} \langle H_D(R, \theta) \rangle &= \frac{\int_0^{B_{\max}} H(t) dB(R, \theta, t)}{\int_0^{B_{\max}} dB(R, \theta, t)} \\ &= \frac{\int_0^{B_{\max}} H(t) \frac{dB}{dt} dt}{\int_0^{B_{\max}} \frac{dB}{dt} dt} = \frac{\int_0^{B_{\max}} H(t) C_L V_D(R, \theta, t) dt}{\int_0^{B_{\max}} C_L V_D(R, \theta, t) dt} \end{aligned} \quad (1)$$

$$\begin{aligned} C_L &= F(R, B(t), \theta) \\ &\approx C_0(R, \theta) + C_1(R, \theta) c \mu t + C_2(R, \theta) c^2 \mu^2 t^2 + \dots, \end{aligned} \quad (2)$$

where, C_L denotes the efficient leakage coefficient of the emf in the pick-up coil for the dB/dt defined as $C_L V_D = -dB/dt$ and μ , the permeability of the material. It is apparent that C_L automatically vanishes if the leakage coefficient is constant during the field sweep. Here, as an approximation, C_L is supposed constant by taking the first term in Eq.2.

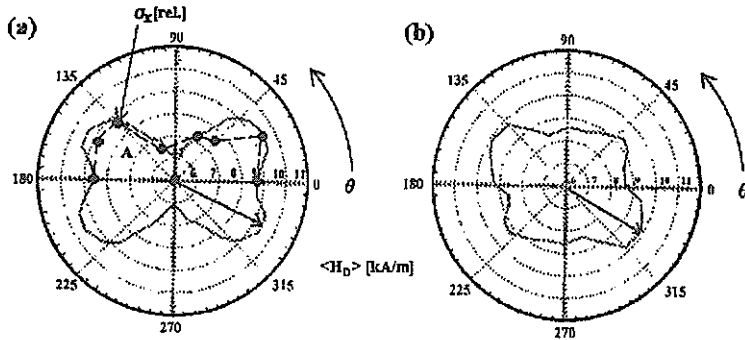


Fig. 6 $\langle H_D('c', \theta) \rangle$ and residual stress σ_x as a function of angle θ for the sample No.1. (a) $\langle H_D('c', \theta) \rangle$ and (b) $\langle H_D('j', \theta) \rangle$

Now it is apparent that, if we adopt the first term of Eq.2, $\langle H_D \rangle$ does not depend on the leakage flux change amplitudes, but it depends on the flux change profile as a function of the field strength up to the maximum field at which saturation magnetization occurs. Fig.6 shows the angle dependence of $\langle H_D(R, \theta) \rangle$ at the two points $R='c'$ in the Lüders band and $'j'$ in the corner of sample No.1, respectively. As shown in Fig. 6(a), $\langle H_D('c', \theta) \rangle$ has a maximum around at 35 degree to stretched direction in the Lüders band and the smallest around at 90 degree. The symmetric properties of the profile with respect to the angle about 90-270 degree must be noted in the present experimental method. Fig.6(b) shows the behavior of $\langle H_D('j', \theta) \rangle$ where a little deformation occurs as a reference point like a virgin state. Apparently, it depends on rectangular against the applied stress direction. Namely, $\langle H_D('j', \theta) \rangle$ is small in parallel and normal directions against the applied stress. The closed circles

in Fig. 6(a) denote the residual stresses observed by XRD at the point "c" in a linear scale (e.g. at an angle of 135 deg. in this figure, $\sigma_x = 15$ [kgf/mm²]). As it is evidently noticed, the closed circles follow almost linearly with the solid curve of $\langle H_D \rangle$, which suggest the linear relationship between σ_x and $\langle H_D \rangle$. The physical meaning of the derived value will be discussed in the next section.

3. DISCUSSION

The physical interpretations of the leakage flux distribution have already analyzed by the present authors and explained in the reference elsewhere [8]. In this discussion, therefore, we deal with the physical meaning of $\langle H_D \rangle$ and its validity as an degradation indicator.

We observed the induced voltage in the pick-up coil, caused by discontinuous magnetizations. In this paper, we adopt a model of domain wall jumps [5]. A magnetic domain wall is pinned by numerous dislocations, defects, and/or voids. For simplicity we adopt here a quasi linear model for a single grain and where a pinning force $f_i(x)$ of the i 'th domain at a position x is caused by an edge or a screw dislocation as expressed by

$$f_i(x) = \pm b\ell [C_1 \sin^2 \frac{2\pi}{\delta}(x - x_p) + C_2 \sin \frac{2\pi}{\delta}(x - x_p)]. \quad (x_p < x < x_p + \delta). \quad (3)$$

Here b, ℓ, δ denote the length of the Burgers vector, the length of dislocation and the thickness of the domain wall, respectively. x_p denotes a different pinning position up to N_p ($p=1, 2, \dots, N_p$). C_1 and C_2 denote numerical factors ranging 1.0~7.0 for edge and screw dislocations of this material. The sign of \pm corresponds to the drag and pushing forces, respectively. The equilibrium condition between the force F exerted by the magnetic field H on a magnetic domain wall with numerous pinning points is given by

$$\begin{aligned} F(x_d) &= 2H \cdot m(x_d)S_D \\ &= \sum_{i=1}^{N_p} f_i(x_d) \end{aligned} \quad (4)$$

Here, $m(x_d)$ denotes the magnetization with a de-pinning position x_d of the magnetic domain with the cross section S_D in a magnetic field H . H increases discontinuously at $t=t_k$ ($k=1, 2, \dots, K$; $H_k < H_{k+1}$, $x_d^{(k)} < x_d^{(k+1)}$) for an external linear sweep with an incremental magnetization between the sequential de-pinning as

$$\begin{aligned} F(x_d^{(k)}) &= 2H_k \cdot m(x_d^{(k)})S_D, \\ \Delta m(x_d^{(k)}) &= m_S S_D (x_d^{(k)} - x_d^{(k-1)}) \end{aligned} \quad (5)$$

Where, we supposed a constant domain wall cross section S_D for any de-pinning processes. Note here that $x_d^{(k)}$ changes discontinuously with time elapses and rather it behaves like a random walk within a semi-local position R as $x_d^{(k)} < x_d^{(k+1)} \in R$ within the theoretical frame of 1-D picture. On the other hands, $V_d(t_k)$ is expressed as

$$\begin{aligned} V_d(t_k)\Delta t_k &= n \left[\frac{d(S \cdot B)}{dt} \right]_{t=t_k} \Delta t_k \approx C_L \frac{\Delta m_k(r_D^{(k)})}{\Delta t_k} \Delta t_k, \\ \Delta t_k &= t_k - t_{k-1} \end{aligned} \quad (6)$$

Here, $n[\dots]_{t=tk}$ denotes the emf caused by the leakage flux change in the pick-up coil with n -turns, which is tentatively supposed proportional to the internal flux change in Eq. 6 with a coefficient C_L and independent on H . Here we discuss more rigorously on the geometry and the inhomogeneity around the pick-up coil. By using Eq. 4, 5 and 6, the average magnetic field $\langle H_D \rangle$ in Eq. 6 is now approximated by taking the first term in Eq. 2, which is possible by choosing an appropriate pick-up coil position R or at an off-center position in between the two poles. The equation of $\langle H_D \rangle$ is now calculated in terms of magnetization m and magnetic field H instead of Eq. 1 as

$$\langle H_D(\mathbf{R}, \theta) \rangle = \frac{\sum_{k=1}^K C_L H_k V_D(t_k) \Delta t_k}{\sum_{k=1}^K C_L V_D(t_k) \Delta t_k} = \frac{\sum_{k=1}^K \mathbf{H}_k \cdot \Delta \mathbf{m}(x_d^{(k)})}{\sum_{k=1}^K \Delta \mathbf{m}(x_d^{(k)})} \quad (7)$$

Here, the nominator of the third equation is expressed as

$$\begin{aligned} \mathbf{H}_k \cdot \Delta \mathbf{m}(x_d^{(k)}) &= \mathbf{H}_k \cdot [\mathbf{m}(x_d^{(k)}) - \mathbf{m}(x_d^{(k-1)})] \\ &\approx [F_k(x_d^{(k)}) - F(x_d^{(k-1)})] / 2S_D - \Delta \mathbf{H}_{k-1} \cdot \mathbf{m}(x_d^{(k-1)}) \end{aligned} \quad (8)$$

Therefore, we obtain an equation for a discontinuous magnetization energy [3] as

$$\begin{aligned} E_D(R, \theta) &= \sum_{k=0}^K [\mathbf{H}_k \cdot \Delta \mathbf{m}(x_d^{(k)}) + \mathbf{m}(x_d^{(k-1)}) \cdot \Delta \mathbf{H}_{k-1}], \quad (= \int d(\mathbf{H}\mathbf{m}) = H_{\max} m_S S_D x_D) \\ &= \sum_{k=0}^K [F(x_d^{(k)}) - F(x_d^{(k-1)})] / 2S_D = F(R, \theta) / 2S_D, \\ &[F(R, \theta) \equiv F(x_d^{(K)}) \quad , F(x_d^{(0)}) = 0, \quad x_D \equiv |x_d^{(K)} - x_d^{(0)}|] \end{aligned} \quad (9)$$

We obtain $\langle H_D(R, \theta) \rangle$ as an average field for a sample composed of numerous grain number up to J , for which the pick-up coil can detect the sequential signals at separate times. Now, the physical quantity of $\langle H_D(R, \theta) \rangle$ is given for a total sample by substituting Eq. 8 and 9 as

$$\langle H_D(R, \theta) \rangle = H_{\max} - \sum_j \left\{ \frac{\sum_{k=0}^K (x_{dj}^{(k)} - x_{dj}^{(0)}) \cdot \Delta \mathbf{H}_{kj}}{x_{Dj}} \right\}, \quad (10)$$

$$= \sum_j \left\{ \sum_{k=0}^K \frac{\Delta x_{dj}^{(k)}}{x_{Dj}} \cdot \mathbf{H}_{kj} \right\} \quad (11)$$

Note here that the quantity in Eq. 11 is independent of the amplitude of emf in the pickup coil, or at least, weakly dependent on the geometry changes with the pick-up coil shifts. The physical meaning of $\langle H_D(R, \theta) \rangle$ is now clarified that the field H_k is weighted with the normalized jump distance of the domain wall. Therefore, $\langle H_D(R, \theta) \rangle$ increases with increasing the field range where domain jumps frequently occur. In other words, if jumps do not cease in the stronger

field, $\langle H_D(R, \theta) \rangle$ increases with increasing the field for saturation magnetization. This phenomena is consistent with the interpretation that the degree of degradation become larger in accordance with the larger density of lattice imperfections or pinning center density. For the larger density of pinning centers caused by lattice imperfection and their segregation, the depinning force become larger. Further, it is easy to extend the 1-Dimensional model to 3-Dimension by replacing a vector position r instead of a scalar x in Eq.6 and Eq.11, by which the angle dependence of $\langle H_D(R, \theta) \rangle$ could be more explicitly expressed.

As is mentioned before, the physical origin of the locally different leakage flux distribution had been developed by one of the present research group [8]. Following his theory, the different local remanence ρ_m is originated by the induced anisotropy at each point. The linear relationship between the local remanence (residual magnetization) and the residual stress is experimentally determined for this material as

$$\rho_m = -0.0013\sigma_x + 0.86[T] \quad (12)$$

Using this relationship and the Gauss law with boundary condition at the surface, we can simulate the spatial distribution of leakage flux at the surface and the resolution as a function of lift-off distances of the Hall sensor as a forward problem [9].

4. CONCLUSIONS

We investigated on NDE of iron-based material using conventional tools of Hall sensor and a pick-up coil for the availability in the real working places. Especially, the spatial resolution of the degradation using a Hall sensor is more excellent than that by SQUID. The linear relationship between the residual stress and the average field defined in this paper has a good indicator of the degradation. The assumption of the constant C_0 in Eq. 1 is an enough approximation to determine $\langle H_D(R, \theta) \rangle$ for degradation estimations.

ACKNOWLEDGEMENTS

The present authors would like to thank to Prof. Takahashi, Prof. Echigoya, Iwate University Prof. Miya, University of Tokyo and Dr. Kasai, Electro-technical Laboratory for their useful discussions. We are also grateful to the scientific foundations for our investigations supported by Japanese Society of Applied Electromagnetism and Mechanics, Nuclear Fuels Co. Ltd. and Japan Atomic Energy Research Institute.

REFERENCES

- [1] Harold Weinstock, IEEE Trans. Magn. Vol. 27,1991,pp3231-3236
- [2] A. Cochran, John C. Macfarlane, Luke N.C. Morgan, Jan Kuznik, Ronald Weston, Ling Hao, Robert M. Bowman, Gordon B. Donaldson, IEEE Trans. Appl. Supercond. No.4,1994,pp128-
- [3] Jiles, NDT International Vol.21, No.5, 1988, pp311-319
- [4] R. Ranjan, O. Buck, R.B. Thompson, J. Appl. Phys Vol.61,1987, pp3196-3201
- [5] K. Yamada et. al., Studies in Appl. Electromag. and Mech.13, IOS Press, 1998,pp153-157
- [6] H.Trauble, *Moderne Probleme der Metallphysik*, Bd.II., Ed.A.Seeger, Springer-Verlag, Berlin,1966
- [7] J.Weertman and J.R.Weertman, Physical metallurgy, Ed.R.W.Chan and P.Haasen, North-Holland, Amsterdam, 1983

- [8] Shinnichi Shoji, Doctor Thesis, Saitama University, April 1999.
- [9] K. Yamada et.al. to be presented at Int. Conf. Nucl. Eng. (ICONE-7), Tokyo, Japan, April 20, 1999